Appl Nanosci (2016) 6:913–922
DOI 10.1007/s13204-015-0497-4

ORIGINAL ARTICLE

Synthesis of nanostructured framework of novel $ZnBaO_2$ nanopowder via wet chemical approach and hepatocytotoxicity response

Taimur Athar[1] · Sandeep Kumar Vishwakarma[2] · Razzaq Alabass[1] · Ahmed Alqaralosy[1] · Aleem Ahmed Khan[2]

Received: 24 July 2015 / Accepted: 25 August 2015 / Published online: 4 September 2015

Abstract Wet synthetic process is an effective and facile method at low cost, environmentally benign process for easy scaling-up and then used for fabrication of multi-utility devices. Self-assembling of nanobrick leads to architecture framework with new functional properties which help to make its vast applications as nanodevices with their intrinsic shape, size and functional properties. The bimetallic oxide nanostructure with phase structure was characterized by FTIR, UV–visible electronic absorption, XRD, thermal studies, SEM, TEM, DLS and fluorescence. Nanocrystalline $ZnBaO_2$ powder can be used due to its chemical stability and excellent transmission in the visible region. It was observed that the annealing rate plays an important role to redefine the structural and other physicochemical properties which finally help to change gel into crystalline functional properties with porosity. Wet chemical approach can be used for the synthesis of other metal oxide nanopowders which can be easily scale up for production level. Along with synthesis and characterization, we also assessed biological responses of human hepatocytes exposed to $ZnBaO_2$ nanopowder. Cell membrane permeability and ammonia detoxification were investigated against various concentrations of nanoparticles on in vitro cultured hepatocytes. Our results suggest that low concentrations (<40 μg/ml) of $ZnBaO_2$ nanopowder have no cytotoxic effect on hepatocytes viability, proliferation and detoxification, whereas concentrations above 40 μg/ml depict significant toxicity on cells.

Keywords Soft synthesis · Bimetallic oxide · Nanostructural · Physicochemical properties · Hepatocytotoxicity

Introduction

Synthesis of homogenously well-dispersed nanostructured metal oxide powder has attracted the attention due to their vast applications in our daily life based on novel physicochemical properties due to their defect chemistry, porosity, surface effects and its quantum confinement effects. To adopt a facile and green strategy for reliable and reproducible synthesis without phase separation remains an open challenge to nanochemists. The ability to control the particle size, shape, surface structure and morphology which play a crucial role both from functional and technological research perspective still remains challenging task. Synthesized $ZnBaO_2$ nanopowder is a new material in the metal oxide series. The wet chemical method is used for its simplicity, low cost and use of non toxic solvents and gives crystalline reproducible yield at moderate conditions with controlled stoichiometric ratio without phase separation and ill-defined particle aggregations. It was observed that the homogenous distribution of bimetallic oxide depends on experimental conditions, type of molecular precursor

✉ Taimur Athar
taimurathar2001@gmail.com

✉ Aleem Ahmed Khan
aleem_a_khan@rediffmail.com

[1] OBC, CSIR-Indian Institute of Chemical Technology, Hyderabad, Andhra Pradesh 500007, India

[2] Salar-E-Millat Research Centre and Central Laboratory for Stem Cell Research and Translational Medicine, Centre for Liver Research and Diagnostics, Deccan College of Medical Sciences, Hyderabad, Andhra Pradesh, India

used and controlled calcinations. The presence of two non-toxic elements helps to maintain colloidal stability under physiochemical condition in human cell for its wide use in screening at the particular pH, which depends on favorable shape and size retaining the surface morphology intact. The use of $ZnBaO_2$ nanopowder has become a motivating area for research due to its volume–cost-effective relation with the macroscopic quantum tunnel effect (Trusova et al. 2012; Hayashi and Hakata 2010; Cao and Wang 2004; Vollath 2008; Lalena and Cleary 2010; Fan et al. 2015; Klabunde and Richards 2012; Muller et al. 2007; Betke and Kickelbick 2014; Athar 2008; Kickelbick and Schubert 2002; Prechtl and Campbell 2013; Naumann 2009; Mackenzie and Bescher 2007; Edler 2004; Klein 1988; Talapin 2012; Lee et al. 2013; Pang et al. 2013; Wang et al. 2005; Pilenic 2007).

It is assumed that due to non-toxic effect of Zn and Ba metal ions, it can be used for sensor and biological applications. However, these fundamental benefits could predictably correlate with changes in the biological properties of the cells. Based upon the analyses of cell adhesion, relative viability, proliferation and functional detoxification assays of human primary hepatocytes during exposure to $ZnBaO_2$ nanoparticles for 72 h, we intended to find its biological safety for biomedical applications. All these considerations are broadly characterized and included in this paper.

Experimental procedures

The structural parameters play a crucial role in determining and optimizing the sensor-related properties (Calfen and Mann 2003; Tretyakov 2003; Rawle 2007; Perry and Carter 2006; Evans et al. 2010; Colfen and Antonietti 2005; Demortière et al. 2008; Shevchenko et al. 2006; Koziej et al. 2014; Ansari et al. 2014). In order to achieve desired shape and size with enhanced functional properties, bottom-to-top wet chemical approach was undertaken to synthesize functional nanopowder for their chemical and biological studies.

Characterization

FTIR spectra were recorded in the range of 4000–400 cm^{-1} using KBr pellets in Perkin–Elmer GX spectrometer with a wave number resolution of 4 cm^{-1}. The optical properties were recorded by using GBC UV–Vis Cintra spectrophotometer with wavelength ranging from 200 to 800 nm. Thermal analysis was carried out by heating the sample at the rate of 10 °C/min from ambient to 1000 °C in dry air using Mettler Toledo star analyzer. X-ray powder diffraction patterns were taken in reflection mode of CuK_α ($\lambda = 1.5406$ Å) radiation from 0θ to 80θ on a Siemens D5000 X-ray diffractometer by using continuous diffraction. Scanning microscopy image was taken by using Hitachi S520 scanning electron microscope. Philips Tecnai G^2 FEI F12 transmission electron microscope was operated at 80–100 kV. The samples were collected on a carbon holey copper grid to see morphology and particle size.

DLS and laser Doppler velocimetry were used for the characterization of particle size and zeta potential in solution by using Malvern Instruments Zetasizer Nano-ZS instruments equipped with 4 mW He–Ne laser $\theta = 632.8$ nm. Steady-state emission spectra were measured using a Shimadzu RF 510 spectrofluorophotometer connected to a Haake Ultra thermostat (Julabo F10) with temperature precision ±0.1 °C using a rectangular quartz cell of dimensions 0.2 cm × 1 cm to minimize the re-absorption.

Materials

Zinc chloride (97 %), barium hydroxide octahydrate (97 %) and solvents were purchased from Aldrich and used as such without further purification. Deionized water with an electrical resistivity of 18 $M\Omega^{-1}$ cm (Millipore, India) was used in the reaction.

Synthesis

Colloidal and monodispersable $ZnBaO_2$ was synthesized via chimie douce. The $ZnCl_2$ (5.74 g, 42.08 mmol) was dissolved in 25 ml deionized water and then heated with stirring from 25 to 130 °C for 6 h. No change in color was observed at neutral pH. The flask was cooled to room temperature, followed by the addition of $Ba(OH)_2{\cdot}8H_2O$ (13.29 g, 42.12 mmol), and again refluxed for 6 h with stirring. The progress of reaction was monitored with the help of pH. The pH remains unchanged 7.5, and it was filtered and a crystalline white powder was obtained after several washing with deionized water. After calcinations, 2.44 g of white powder was obtained. The nanopowder is UV active, and its fluorescence gives butter color.

$$ZnCl_2 + 1.15\ Ba(OH)_2.\ 8H_2O \xrightarrow[\text{Stirring}]{\text{Refluxing}} ZnBa(HO)_2 + 2HCl + 8H_2O$$

$$ZnBa(HO)_2 \xrightarrow{\text{calcination}} ZnBaO_2 + H_2$$

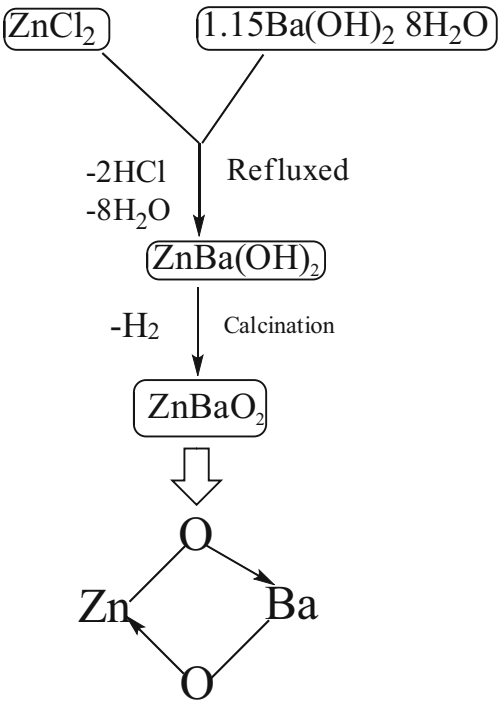

A graphical stretch of the reaction

In vitro cytotoxicity assessment of $ZnBaO_2$ nanoparticles

In this study, we used primary human hepatocytes for in vitro investigation of $ZnBaO_2$ nanoparticles for its cytotoxicity effects. Different biological methods were applied to measure the cellular parameters during nanoparticles exposure and compared with control. Each parameter was validated in triplicate and repeated at least three times.

Hepatocytes culture and $ZnBaO_2$ nanoparticles exposure

Primary human hepatocytes were cultured as previously described (Vishwakarma et al. 2014). Briefly, 2×10^4 cells were cultured on 0.2 % gelatin-coated six-well plates in serum-free medium containing 20 ng/ml epidermal growth factor (EGF; PeproTech, London, UK), 10 ng/ml basic fibroblast growth factor (b-FGF; PeproTech), 20 ng/ml hepatocyte growth factor (HGF; Sigma, St. Louis, MO, USA) and 0.61 g/l nicotinamide (Sigma) with 100 U/ml penicillin G and 100 µg/ml streptomycin sulfate. Cells were maintained in the appropriate culture medium at 37 °C, 95 % humidity and 5 % CO_2. After reaching to 70–80 % confluency, cells were harvested by trypsinization and cultured in respective plates with and without nanoparticles for 72 h in the above-mentioned culture conditions. Cells without nanoparticles were considered as control.

Relative cell viability

Relative cell viability was measured by MTT [3-(4,5-dimethylthiazol-2-yl)-2,5-diphenyltetrazolium bromide] assay which was further validated by trypan blue exclusion assay after 24, 48 and 72 h of exposure to $ZnBaO_2$ nanoparticles at different concentrations ranging from 10 to 100 µg/ml (Athar 2015). The viability was checked after plating the cells with and/or without nanoparticles and incubating them for 72 h.

Cell adhesion assay

In the adhesion assay at 4 h after plating the cells, we estimated the number of cells adhered on the culture plate.

Cell adhesion assay was carried out by plating 2×10^4 cells along with $ZnBaO_2$ nanoparticles on 0.2 % gelatin-coated coverslips and incubating them for 4 h. After 4 h of incubation, non-adherent cells were removed and 50 µl of 1 mg/ml MTT solution was added to the remaining cells and then incubated at 37 °C, 5 % CO_2 and 95 % air conditions for 4–5 h. The reaction was stopped by adding 100 µl of acidified isopropanol. The percentage of cell adhesion was calculated by taking absorbance at 570 nm by using a microplate reader (BioRad).

Cell proliferation assay

Hepatocytes proliferation was measured by using MTT cell proliferation assay. Briefly, 2×10^4 primary human hepatocytes were mixed with $ZnBaO_2$ nanoparticles in variable concentrations as described above and cultured in a 96-well culture plate coated with 0.2 % gelatin. Cells were maintained in serum-free medium under standard condition as described in previous sections. Each variable was kept in triplicate for 24, 48 and 72 h. At each time point, 50 µl of 1 mg/ml MTT was added and incubated for 4–5 h. After incubation, purple formazan crystal was dissolved using 100 µl acidified isopropanol. Absorbance was measured at 570 nm and compared with the control.

LDH activity measurement

$ZnBaO_2$ nanoparticles cytotoxicity on membrane organization was assayed by the amount of lactate dehydrogenase (LDH) released from dead cells using LDH assay kit (Promega, WI). For 24, 48 and 72 h, 2×10^4 viable hepatocytes were incubated with 100 µl of $ZnBaO_2$ nanoparticles (10–100 µg/ml). It was then mixed with 50 µl of reagent. The mixture was incubated for 30 min at room temperature. The reaction was stopped by adding 50 µl of stop solution. Absorbance was measured at 490 nm using a microplate reader (BIORAD). Total cell lysate was used as positive control to assess kit sensitivity for 100 % with the release of LDH from the dead cells after incubation.

Detoxification functional assay

Functional toxicity of $ZnBaO_2$ nanoparticles was assessed by using detoxifying functional assay with NH_4Cl as a source for NH_3 in human hepatocytes. After exposure of dispersed $ZnBaO_2$ nanoparticles, 2.5 mM NH_4Cl was used to assess the rate of ureagenesis in cultured human hepatocytes. The influence of nanoparticles concentration was tested for exposure to 10–100 µg/ml concentrations for 24, 48 and 72 h during in vitro proliferation. Briefly, one million human hepatocytes were incubated with different concentrations of $ZnBaO_2$ nanoparticles for 72 h and used to estimate the efficiency of NH_4Cl detoxification. Briefly, after finishing the incubation with nanoparticles, culture supernatants were collected from each group and then centrifuged at $5000 \times g$ for 5 min to obtain a cell-free supernatant. Urea formation was detected by urease method using a commercial kit (SIGMA).

Statistical analysis

All data were expressed as mean ± standard deviation. Results were compared by one-way and two-way analysis of variance (ANOVA) followed by Dunnett's multiple comparison test. A value of $p < 0.05$ was considered statistically significant.

Results and discussion

Understanding the effect of electronegativity and ionization potential of metal ion helps to control the kinetic–thermodynamic parameters for the formation of primary nuclei and leads to growth process via self-assembly of nanobricks. The synthesis was carried out at moderate temperature by using single-source molecular precursor (Athar et al. 2015a, b, c, d, e; Wang 2000a, b; Mishra et al. 2007).

FTIR

The study was carried out after calcinations, thereby supporting the formation of self-assembled framework by observing the strong Zn–O–Ba symmetric and asymmetric peaks at 498.97 and 851.51 cm^{-1}, respectively. After, there is no significant peak at the range from 1000 to 400 cm^{-1}, which supports the formation of particle after calcinations with purity. At 1000 °C all the surface impurities were removed. Bending vibration of Zn–O–Ba occurs at 1421–61 cm^{-1}, and formation of nanostructure framework takes place by retaining the nanopowder purity. The presence of symmetric and asymmetric peaks at 356 and 1750 cm^{-1} occurred due to absorption of atmospheric moisture during sample preparation. However, it presumed that nanostructure framework is retained without any change in shifting of frequencies after aging as shown in Fig. 1 (Pavia et al. 2009; Skoog et al. 2007; Stuart 2004).

UV studies

UV–Visible spectra were recorded in MeOH to study their electronic properties along with crystalline structure. The presence of excitonic absorption band at 214.4 nm and occurrence of broad transmittance peak at 257.6 nm can be assigned to π–π^* and π–p bathochromic shift, which

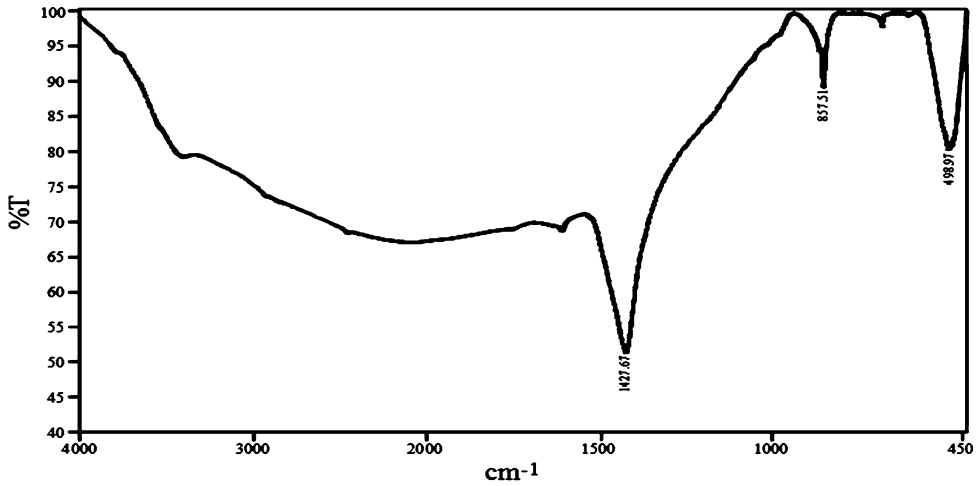

Fig. 1 FTIR study of $ZnBaO_2$ nanoparticles

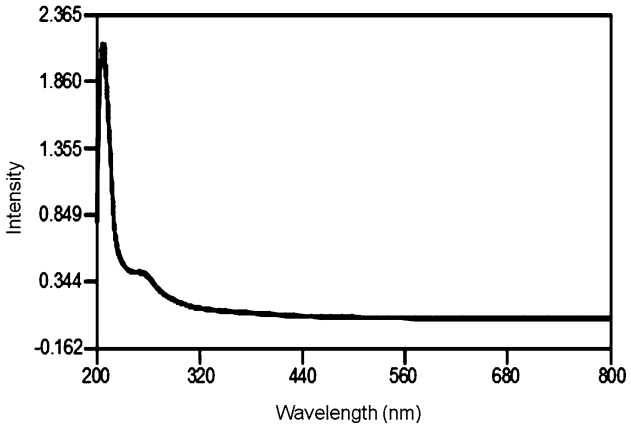

Fig. 2 UV-visible spectra of $ZnBaO_2$ nanoparticles

support the formation of monodispersable colloidal powder with well-defined nanostructured framework due to quantum size effect, which leads to control the surface morphology to enhance functional properties. Controlling the kinetic–thermodynamic parameters helps to shift bathochromic wavelength in the presence of lone pair of electron present in the bridging oxygen atom in between two different metal ions and leads to stabilization of electronic state from the ground state. The formation of self-assembled nanostructured gives crystalline shape due to quantum size effect and oxygen vacancy by using two different metal ions. As the particle size increases, the significant shifting of band occurs, thereby reducing the forbidden band due to the absence of defective surface morphology which leads to aggregation due to primary nucleation without effecting the chemical composition as shown in Fig. 2 (Skoog et al. 2007; Stuart 2004; Gabbott 2007).

XRD studies

The presence of strong diffraction peaks confirms the formation of crystalline structure of nanostructure $ZnBaO_2$ framework. The particle size was calculated with the help of Bragg–Scherer's equation. It is difficult to assign diffraction peaks, because it is a new nanopowder, so far not reported in JCPDS data file. The presence of sharp peaks supports the formation of crystalline phase. The particle size was calculated by using Scherer equation and found to be 15.88 nm. All peaks can be assumed by assigning index to hexagonal phase, and no other phase was observed supporting the high purity of the sample as shown in Fig. 3 (Skoog et al. 2007; Stuart 2004; Mitra 2003; Guinier 1994).

Thermal studies

The thermal analysis was carried out to understand the changes taking place in the particle shape, size, morphology and texture chemistry after the removal of surface impurities to give right prediction of physical properties. Thermal studies help in getting the information of how crystalline particle was built via self-assembly. The first step involves the removal of unbound water at 85 °C and then followed by removal of other volatile materials at 170 and 210 °C. Thereafter, formation of crystalline powder takes place as supported by no further change in weight. The same information was obtained from DTA studies. It is concluded that the formation of phase strongly depends on the type of molecular precursor used, mode of synthetic methodology and polarity of solvent. The detailed analysis is shown in Fig. 4 (Skoog et al. 2007; Stuart 2004; Mitra 2003; Gabbott 2007).

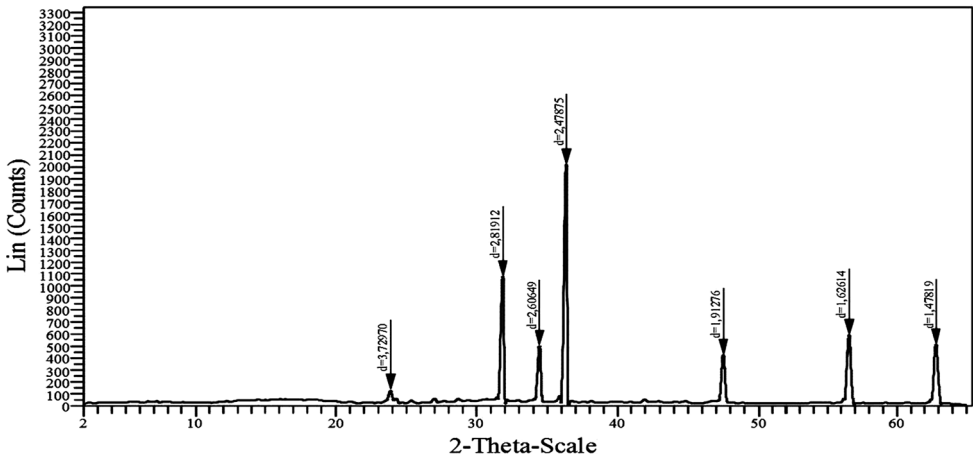

Fig. 3 XRD study showing strong diffraction peaks which confirm the formation of crystalline structure of nanostructure $ZnBaO_2$ framework

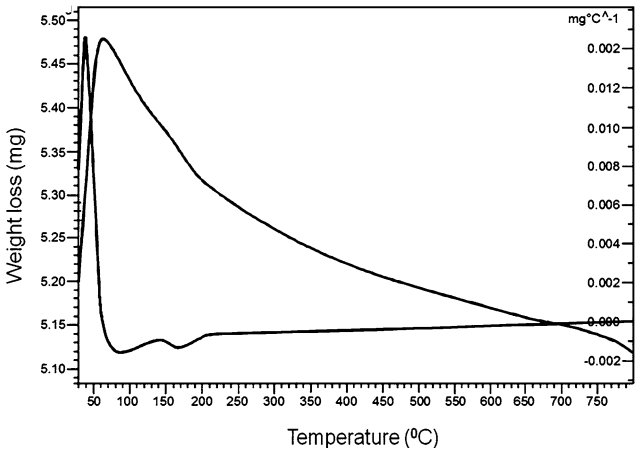

Fig. 4 Thermal study showed that formation of phase strongly depends on the type of molecular precursor used, mode of synthetic methodology and polarity of solvent

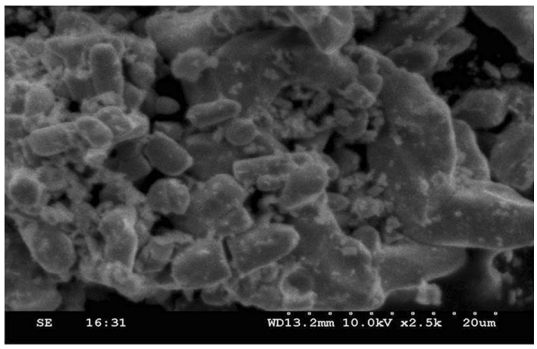

Fig. 5 SEM image of $ZnBaO_2$ nanoparticles shows granular, well-dispersed, *square* and *flake-like* structure

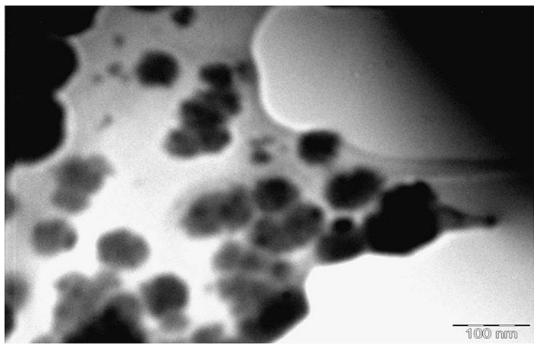

Fig. 6 TEM image $ZnBaO_2$ nanoparticles shows granular non-spherical round and smooth particle with different particle morphology

SEM studies

The shape of $ZnBaO_2$ nanopowder obtained was granular and well dispersed with a square shape. SEM images show flake-like structure due to inter- and intramolecular forces with limited porosity. The small particle interaction takes place due to Ostwald ripening process and with high surface energy as shown in Fig. 5 (Mitra 2003; Davydov 2003; Zeng 2007).

TEM studies

TEM investigation gives information about the structural and morphological features of nanoparticles. TEM image shows granular, non-spherical, round and smooth with different particle morphology due to aggregation after annealing and the presence of high surface energy with narrow particle size distribution. The nanoparticle agglomerates into several other primary particles which can be classified as secondary particles due to the presence of soft forces as well as hard forces as shown in Fig. 6 (Mitra 2003; Davydov 2003; Zeng 2007; Wang 2000a, b).

DLS studies

DLS studies were preformed with scattering of light intensity with reference to time due to random Brownian motion which leads to stability of suspended particle size in

water. The mean particle size diameter was found to be 300 nm as shown in Fig. 7 (Jillavenkatesa et al. 2001; Brillain 2001).

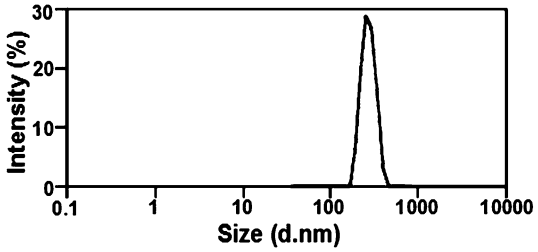

Fig. 7 DLS study of $ZnBaO_2$ nanoparticles

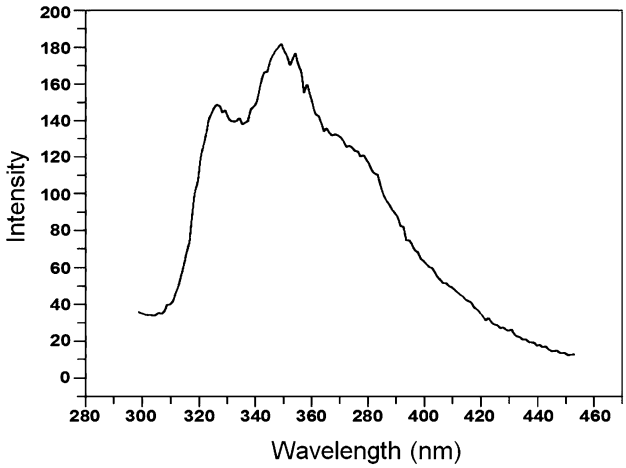

Fig. 8 Fluorescence studies of $ZnBaO_2$ nanoparticles exhibited broad excitonic peak at 322 and 351 nm with excitation intensity (*Y*-axis) at 150 and 180 giving information of nanostructure framework

Fluorescence studies

The fluorescence studies exhibit the presence of broad excitonic peak at 322 and 351 nm with excitation intensity (*Y*-axis) at 150 and 180 to give information about the formation of nanostructure framework with purity. The excitation intensity changes with temperature; however, intrinsic intensity remains constant with concentration. The following observation can be assumed: (1) the shape and band maxima of absorption and fluorescence spectra remain unchanged, (2) no other type of emission band was observed and (3) finally absorbance of the fluorophore does not change during experiment as shown in Fig. 8 (Lakowicz 2006).

Cell adhesion and changes in cell viability during exposure to $ZnBaO_2$ nanoparticles

Relative cell viability and adhesion assays on human hepatocytes were performed using protocols described in Materials and methods, and the results are shown in Fig. 9a, b. During cell adhesion assay at 4 h after plating the cells, we could estimate that almost 80 % cells were adherent in control and nanoparticles were exposed to the cell with a concentration of 30 µg/ml. However, it was gradually decreased above 40 µg/ml and was significantly reduced at higher concentrations (Fig. 9a).

Relative cell viability percentage was calculated for 24, 48 and 72 h of nanoparticles exposure to hepatocytes. Figure 9b shows that there was no change in cell viability at lower concentration up to 30 µg/ml. But it was significantly reduced with incubation time and increasing nanoparticles concentration. As compared to 24 h of incubation, at 48 h and 72 h significantly reduced viability was observed above 40 µg/ml nanoparticles exposure.

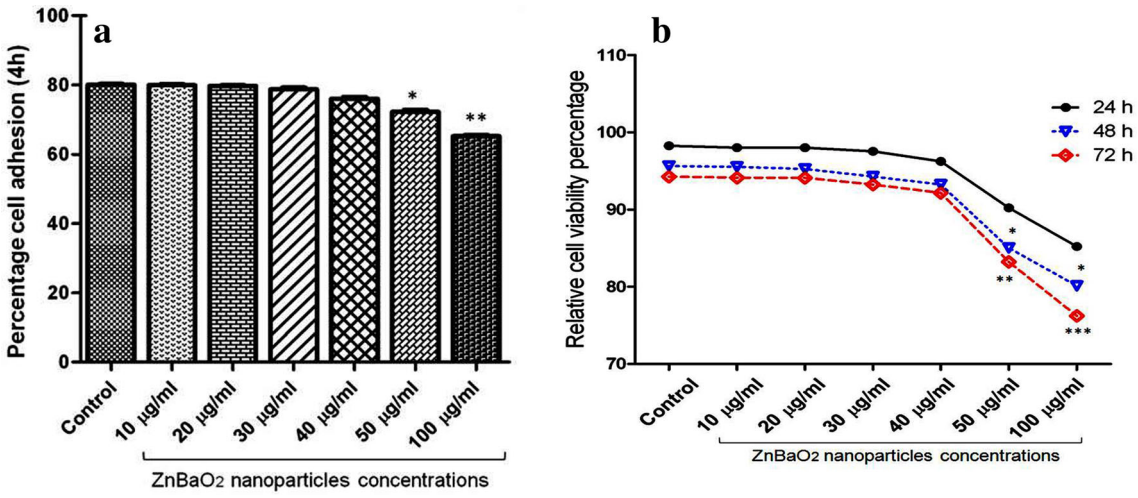

Fig. 9 Effect of $ZnBaO_2$ nanoparticles exposure on **a** cell adhesion after 4 h and **b** relative cell viability at 24–72 h

Assessment of cell proliferation

Cell counts at different time points after plating 2×10^4 cells with and without nanoparticles were estimated, and data are shown in Fig. 10. We observed continuous increase in cell number with time progression. However, proliferation rate of cells was decreased with increasing nanoparticles concentration with respect to time as compared to control which could probably be due to poorer viability of cells exposed to nanoparticles.

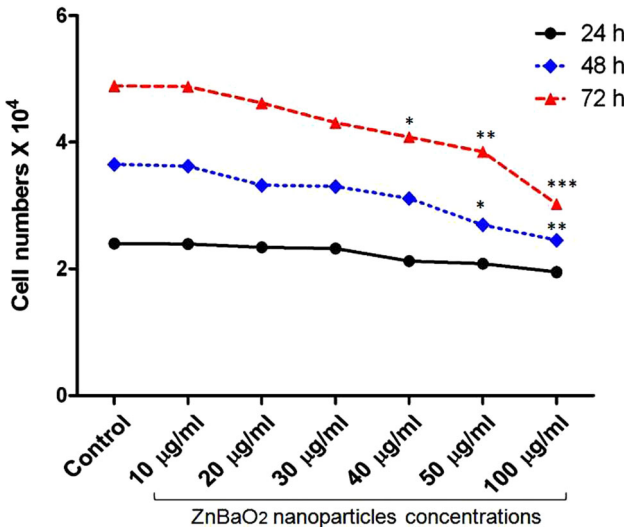

Fig. 10 Changes in cell numbers during hepatocytes proliferation on exposure to different concentrations of $ZnBaO_2$ nanoparticles for 24–72 h

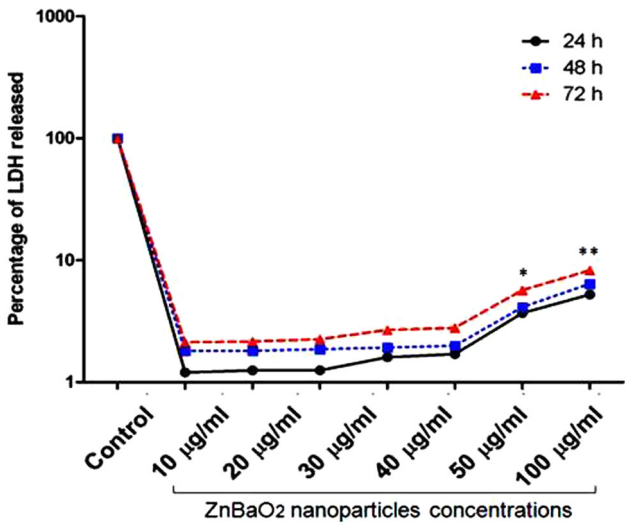

Fig. 11 Effect on cell membrane permeability measured by the release of LDH from cells during exposure to various concentrations of $ZnBaO_2$ nanoparticles

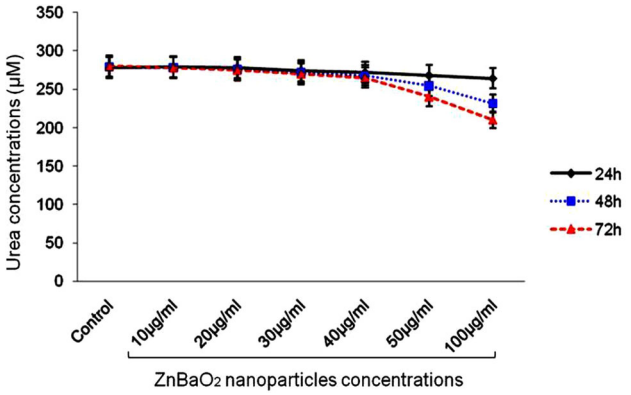

Fig. 12 In vitro ammonia detoxification assay showing changes in urea production after 24-, 48- and 72-h exposure to $ZnBaO_2$ nanoparticles

LDH activity and cell membrane permeability

In vitro LDH assay was performed in human hepatocytes with incubation time of 24–72 h by using $ZnBaO_2$ nanoparticles. Figure 11 shows that there was steady release of LDH from cells treated with low concentration of $ZnBaO_2$ nanoparticles which was almost similar to control up to 30 µg/ml concentration. However, LDH release was enhanced above 40 µg/ml nanoparticles concentrations and was significantly high at 50–100 µg/ml. In general, high concentration of nanoparticles causes LDH leakage from cells representing reduced cell viability as well as cell membrane integrity.

Effect on hepatocytes detoxification

Human hepatocytes when incubated with $ZnBaO_2$ nanoparticles at variable concentrations for 72 h showed decrease in efficiency for detoxification of NH_4Cl in dose-dependent manner (Fig. 12). After 72 h, 100 µg/ml concentration was found to have highest impact on ammonia detoxification. Lower concentrations (<30 µg/ml) did not show adverse effects in hepatocytes.

Conclusions

Wet chemical approach helps to control the size, shape, composition and structural particle properties at the intergrain space which is not oxidized in the air leading to monodispersity with colloidal stability. Right chemical composition and microstructural properties help to fabricate sensor devices. The shape of a building block is the determining factor for structural and functional properties in nanostructure. Synthetic strategies based on topotactic wet chemical approach give information of state-of-the-art

design to enhance functional materials. The wet chemical approach is novel process that does not involve high temperature, so is suitable for bulk production. It was demonstrated that the hepatocytotoxicity depends on varying concentrations of $ZnBaO_2$ nanoparticles exposure at different time points. These nanoparticles may have potential applications in a variety of areas which need to be explored further.

References

Ansari ZA, Khan AA, Fouad H, Athar T, Ansari SG (2014) Application of platinum doped $MnTiO_3$ as electrochemical cholesterol sensor. Sens Lett 12(8):1–5. doi:10.1166/sl.2014.3309

Athar T (2008) Handbook of metal oxide nanopowder. In: Ahmad W, Jackson MJ (eds) Emerging nanotechnologies for manufacturing. William Andrews, Norwich. ISBN: 978-0-8155-1583-8

Athar T (2015) Soft chemical approach for the synthesis and characterization of aluminium copper oxide $CuAl_2O_4$ nanopowder. Adv Mater Lett 6(3):265–270. doi:10.5185/amlett.2015.5659

Athar T, Ansari ZA, Fouad H, Ansari SG (2015a) Soft chemical synthesis of functional $NiSb_2O_4$ nanopowder and its application as hydrazine electrochemical sensor. Arab J Chem. doi:10.1007/s10854-015-3047-7

Athar T, Khan AA, Razzaq A, Ahmed A, Vishwakarma S (2015b) Green approach for the synthesis and characterization of $ZrSnO_4$ nanopowder. Appl Nanosci. doi:10.1007/s13204-015-0488-5

Athar T, Abdelaal M, Khatoon Z, Kumar A, Razzaq A, Khan A, Fouad H, Ansari SG, Ansari ZA (2015c) Green synthesis of $NiSnO_3$ nanopowder and its application as hydroquinone electrochemical sensor. Sens Mater 27(7):563–573

Athar T, Razzaq A, Vishwakarma SK, Bardia A, Habeeb MA, Paspala SAB, Shafi SSM, Khan AA (2015d) Soft chemical approach for the synthesis, characterization and safety assessment of novel Fe_3AlO_6 nanopowder in human neural precursor cells. J Bionanosci 9(2):139–144. doi:10.1166/jbns.2015.1282

Athar T, Khan AA, Vishwakarma SK, Razzaq A, Ahmed A (2015e) A review on synthesis of nanostructured metal oxide powder via soft chemical approach. Rev Adv Sci Eng 4:1–13

Betke A, Kickelbick G (2014) Bottom-up chemical techniques for the continuous synthesis of inorganic nanoparticles. Inorganics 2(1):1–15. doi:10.3390/Inorganics2010001

Brillain HG (2001) Particle size distribution, part E—representation of particle, shape size and distribution. Pharm Tech 25(12):38–45. ISSN: 0147-8087

Calfen H, Mann S (2003) Higher-order organization by mesoscale self-assembly and transformation of hybrid nanostructures. Angew Chem Int Ed 42(21):2350–2365. doi:10.1002/anie.200200562

Cao G, Wang Y (2004) Handbook of nanostructures and nanomaterials: synthesis, characterization and applications, 2nd edn. Imperial College Press, London. ISBN-13: 978-1860944802

Colfen H, Antonietti M (2005) Mesocrystals, Inorganic superstructures made by highly parallel crystallization and controlled alignment. Angew Chem Int Ed 44(35):5576–5591. doi:10.1002/anie.200500496

Davydov A (2003) Molecular spectroscopy of oxide for catalyst surface. Wiley, Hoboken. ISBN: 978-0-471-98731-4

Demortière A, Launois P, Goubet N, Albouy PA, Petit C (2008) Shape-controlled platinum nanotubes and their assembly into two dimensional and three dimensional superlattices. J Phys Chem 112(46):14583–14592. doi:10.1021/jp802081n

Edler KJ (2004) Handbook of sol–gel processing. Kluwer, London. ISBN: 1-4020-7969-9

Evans G, Duong GV, Ingleson MJ, Xu Z, Khimyak YZ, Claridge JB, Rosseinsky MJ (2010) Chemical bonding of multifunctional oxide nanocomposite. Adv Funct Mater 20(2):231–238. doi:10.1002/adfm.200901632

Fan Z, Haung X, Tan C, Zhang H (2015) Thin metal nanostructures: synthesis, properties and applications. Chem Sci 6(1):95–111. doi:10.1039/C4SC02571G

Gabbott P (2007) Principles and applications of thermal analysis. Wiley, Hoboken. ISBN: 13:978-1-4051-3171-1

Guinier PA (1994) X-ray diffraction in crystals, imperfect crystals and amorphous bodies. Dover, New York. ISBN: 0486-68011-8

Hayashi H, Hakata Y (2010) Hydrothermal synthesis of metal oxide nanoparticles in supercritical water. Materials 3(7):3794–3817. doi:10.3390/ma3073794

Jillavenkatesa A, Dapkunas SJ, Lum LH (2001) Particle size characterization. Recommended practical guide. NIST, Washington, DC

Kickelbick G, Schubert U (2002) In: Barton MI (ed) Synthesis, functionalization and surface treatment of nanoparticles, chap 6. American Scientific, Los Angeles, pp 91–102. ISBN: 1-58883-009-8

Klabunde KJ, Richards RM (2012) Handbook of nanoscale materials in chemistry, 2nd edn. Wiley, New York. ISBN: 978-0-470-22270-6

Klein LC (1988) Handbook of sol–gel technology for thin film, fibres, performs, electronic, and specialty shape. Noyes, Park Ridge. ISBN: 0-8155-1154-X

Koziej D, Lawra A, Niederberger M (2014) Metal oxide particles in materials science addressing all length scale. Adv Mater 26(1):235–257. doi:10.1002/adma.03161

Lakowicz JR (2006) Handbook of principle of fluorescence spectroscopy, 3rd edn. Springer, Baltimore. ISBN: 978-0-387-46312-4

Lalena JN, Cleary DA (2010) Handbook of principles of inorganic materials design. Wiley, New York. ISBN: 978-0-470-40403-4

Lee J, Zhang S, Sun S (2013) High temperatures solution phase synthesis of metal oxide nanocrystals. Chem Mater 25(8):1293–1304. doi:10.1021/cm3040517

Mackenzie JD, Bescher EP (2007) Chemical routes in the synthesis of nanomaterials using the sol–gel process. Acc Chem Res 40(9):810–818. doi:10.1021/ar7000149

Mishra S, Daniele S, Pfalzgraf LGH (2007) Metal 2-ethylhexanoates and related compounds as useful precursors in materials science. Chem Soc Rev 36(11):1770–1787. doi:10.1039/B614334M

Mitra S (2003) Handbook of sample preparation techniques in analytical chemistry. Wiley, Hoboken. ISBN: 0-471-32845-6

Muller A, Cheetham AK, Rao CNR (2007) Handbook of nanomaterials chemistry: recent developments and new directions. Wiley-VCH, New York. doi:10.1002/352760247X

Naumann RJ (2009) Introduction to the physics and chemistry of nanomaterials. CRC Press, Boca Raton. ISBN-10: 142006133X

Pang X, Zhao L, Han W, Xin X, Lin Z (2013) A general and robust strategy for the synthesis of nearly monodisperse colloidal nano crystals. Nat Nanotechnol 8(6):426–431. doi:10.1038/nnano.2013.85

Pavia DLGL, Kriz GS, Vyvyan JR (2009) Handbook of introduction to spectroscopy, 4th edn. Cengage Learning, Boston. ISBN-13: 978-0-495-11478-9

Perry CR, Carter B (2006) Insights into nanoparticle formation mechanisms. J Mater Sci 41(9):2711–2722. doi:10.1007/s10853-006-7874-z

Pilenic MP (2007) Control of the size and shape of inorganic nanocrystals at various scales from nano to macro domains. J Phys Chem 111(26):9019–9038. doi:10.1021/jp070646e

Prechtl MHG, Campbell PS (2013) Metal oxide and bimetallic nanoparticles in ionic liquids: synthesis and application in multiphase catalyst. Nanotechnol Rev 2(5):577–595. doi:10.1515/intrev-2013-0019

Rawle AF (2007) Micron sized nanomaterials. Powder Technol 174(1):6–9. doi:10.1016/j.powtec.2006.10.012

Shevchenko EV, Talapin DV, Kotov NA, Brien SO, Murray CB (2006) Structural diversity in binary nanoparticles superlattices. Nature 439:55–59. doi:10.1038/nature04414

Skoog DA, Holler FJ, Crouch SR (2007) Handbook of principles of instrumental analysis, 6th edn. Thomson Brooks, Belmont. ISBN: 0495012017

Stuart HB (2004) Handbook of infrared spectroscopy fundamentals and applications. Wiley, New York. ISBN: 978-0-470-85428-0

Talapin DV (2012) Nano crystal solids, a modular approach to material design. MRS Bull 73(1):63–71. doi:10.1557/mrs.2011.337

Tretyakov YD (2003) Self-organization processes in the chemistry. Russ Chem Rev 72(8):731–763. ISSN: 0042-1308

Trusova EA, Vokhmintcev KV, Zagainov IV (2012) Wet chemistry processing of powdery raw materials for high tech ceramic. Nanoscale Res Lett 7(1):58–61. doi:10.11861/1556-2768x-7-58

Vishwakarma SK, Rahamathulla S, Bardia A, Tiwari SK, Srinivas G, Raj A, Tripura C, Sandhya A, Habeeb MA, Khan AA, Pande G, Reddy KP, Reddy PY (2014) In vitro quantitative and relative gene expression analysis of pancreatic transcription factors Pdx-1, Ngn-3, Isl-1, Pax-4, Pax-6 and Nkx-6.1 in trans-differentiated human hepatic progenitors. J Diabetes Investig. doi:10.1111/jdi.12193

Vollath D (2008) Handbook of nanomaterials. Wiley, New York. ISBN: 978-0-470-40403-4

Wang ZL (2000a) Characterization of nanophase materials. Wiley-VCH, New York. ISBN: 9783527600090

Wang ZL (2000b) Transmission electron microscopy of shape controlled nanocrystals and their assemblies. J Phys Chem 104(6):1153–1175. doi:10.1021/jp993593c

Wang X, Zhang J, Peng Q, Li Y (2005) A general strategy for nano crystal synthesis. Nature 437:121–124. doi:10.1038/nature03968

Zeng HF (2007) Ostwald ripening a synthetic approach for hallow nanomaterials. Curr Nanosci 3:177–181. doi:10.2147/15731307780619279